Chapter-4

Synthesis and Characterization of Ti-Si-Mn alloy- Bioactive glass Composite

4.1 Introduction

Silicon is one of the most common elements on Earth - it occupies the second place after oxygen and is present in most cells, which indicates its necessity for the development of most organisms. Silicon is necessary for the synthesis of collagen and elastin and it is important for the health of the connective tissues, bones, cartilage, tendons and joints. The collagen acts as a scaffold that provides support to the tissues, whereas elastin gives elasticity to the tissues, skin, hair and blood vessels.

Bone is actually a special type of connective tissue. As the bone matures, silicon concentration declines and deposits of calcium and phosphorus are formed at the same time. Therefore, it is concluded that silicon acts as a regulating factor for the deposition of calcium and phosphorus in bone tissue. In addition to connective tissue and bone health, silicon also plays a role in other health benefits such as protection against aluminium toxicity and protection of arterial tissue.

Ti–Si alloy will be the good choice for the implant materials in tissue and damaged organs because of its good biological compatibility. The phase diagram of Ti-Si alloy reveals that the melting temperature of titanium (1670^0 C) decreases with an increasing percentage of Si and reaches approximately 1330^0C at the eutectic composition (8.3 wt % of Si) [19, 20] and can be expected to act as a b-stabilizer (b-eutectoid former). Therefore we can control phase stability, which leads to desirable mechanical and physical properties through an optimal choice of alloy composition and heat treatment route.

Manganese (Mn) is a low-cost material which also reduces α to β transformation temperature of titanium and is considered as a β stabilizer element. It also positively affects the remodeling of the bone, osteogenesis and other functional mechanisms in the body. It has been found in the literature that Mn concentration less than 8 wt % in titanium shows negligible effects on the cell proliferation of osteoblasts cells and on the metabolic activity. So it could be used as an alloying element in a smaller amount for biomedical applications [1, 2].

The production of Ti alloys is difficult because of its high reactivity at elevated temperature as well as the possibility of contamination. Ti alloys production via powder metallurgy (PM) route is preferred because of the ability to produce net-shape components. In powder metallurgy route, the mechanical alloying is achieved by planetary ball mill where high-energy collision occurs among the balls to induce diffusion at the atomic level. This increases the limit of solid solubility in the alloy.

The efforts are being made to improve the osseointegration and host response by altering the surface of the titanium[4], In spite of all the above facts, it is still difficult to achieve a chemical bonding with the bone tissue and form a new bone on its surface. To overcome this issue, the implant surface had been coated with bioactive materials like hydroxyapatite, bioglass, etc. These materials have an excellent capacity to bond with the living tissues [5]. But the problems associated with the coated alloys are poor adhesiveness, non-uniform coating and the difference in the thermal coefficient of the metal substrate and coating material [5].

Bio-active glasses are the richest class of biomaterials which are commonly based on borate, silicate, and amorphous phosphate structures [6]. Hench has invented the first

bioactive silicate glass known as 45S5 Bioglass which has good bonding characteristics with the bone and also encourages the growth of bone [7-8]. The silicate glasses have the slow rate of degradation due to SiO2 rich layer formed within the body, whereas the borate base glass like 1393 B3 has the high rate of degradation because of high leachability [6, 9]. Along with the fast degradation rate, it shows good bioactivity within the cells. However, the low level of strength and brittle nature of glasses puts the limit on its application in soft tissues [10, 11].

Current work comprises the synthesis of newly developed low cost Ti-8Si-2Mn alloy matrix by powder metallurgical route which is reinforced with 1393 B3 bioactive glass in the percentage range of 5 - 20%. Borate bioactive glass has been chosen because of the quick degradation and its conversion into hydroxyapatite. The main aim of current work is to optimize the mechanical and biological properties of 1393 B3 bioactive glass to match the resultant biomechanical properties with the cortical bone and to remove the drawback of coated alloys by incorporating the glass into the matrix.

4.2 Alloy Preparation

Titanium (Ti) metal powder is mechanical alloyed (MA) with eight weight percent of Silicon (Si) and two weight percent of Manganese (Mn) metal powders in a high energy ball mill containing stainless steel vial along with tungsten balls for the synthesis of titanium alloy powder at room temperature. The powder-to-ball weight ratio was maintained at 10:1. The vial of the mill was loaded with powder in an argon-filled glove-box to prevent oxidation.

The mill was run up to 15 h for powder alloy preparation. Because of the ductility of metal powders; the milling is carefully controlled by adding a small amount of process control

agent, (PCA), i.e., two weight % ethanol to the milling process was added. The PCA enhance milling efficiency by refreshing metal surface contacts. It also reduces the welding of the powder particles to each other and prevents the oxidation and contamination of material [12].

4.3 Synthesis of Glass

The glass batch containing following composition 56.6 % B_2O_3,18.5 % CaO, 5.5%Na_2O, 11.1% K_2O,4.6 %MgO,3.7% P_2O5, as weight percentage were prepared taking the starting material as Quartz(99% SiO_2), Magnesium Oxide (99%MgO) Calcium Carbonate (99%$CaCO_3$), Sodium Carbonate (99%Na_2CO_3), Potassium carbonate (98%K_2CO_3) and Boric acid (99%B_2O_3). The materials were mixed for 30 minutes in a mortar pestle. These reagents were then melted in a platinum crucible for 4.5 h in an electric furnace at 1300^0C. Further, the glass melt was water quenched. Resultant glass was crushed and ball milled in the pot mill to bring in the powder form.

4.4 Composite preparation

The mechanically alloyed metal powder matrix was reinforced with 5, 10 and 20 percentage of melt-quenched 1393 B3 bioactive glass and ball milled for 20 minutes for homogeneous mixing, and 0.3 % of carboxyl methyl cellulose (CMC) is added as an organic binder. A uniaxial cold press machine is used to consolidate the composites under the pressure of 450 MPa in the form of bars and pallets. The green compacts were pre-sintered first at 700^0C for 1 h for binder removal and then sintered in a high vacuum tube furnace with the holding time of 4 h at 1250 °C with the heating rate of 10 °C/min. The cooling is achieved first at 10 °C/min till 900°C and then allowed to cool at a faster rate of 40°C/min.

4.5 Result and Discussions

4.5.1 Phase Analysis

Fig. 4.1 shows the X-Ray diffraction pattern of the samples after sintering. The X-ray pattern reveals that metal alloy without bioactive glass (S1) has hexagonal α Ti (PCPDF No 892762) as a significant phase with some sort of BCC β Ti (PCPDF No-894913), Si (PCPDF No 800018) and α Mn (PCPDF No 892412). In addition to alpha and beta titanium, the brittle intermetallic compound Ti¬5Si3 (PCPDF No 893721) also formed. With the reinforcement of bioactive 1393 B3 glass in Ti alloy matrix (S2, S3, and S4), some additional peaks of Ti5P3 (PCPDF No.658413), Ti (Bo3) (PCPDF No.850168) are also observed in the pattern as a reaction between metal and glass constituents. XRD pattern of composite suggests that the intensity of these peaks increases with the weight percentage of reinforced BAG.

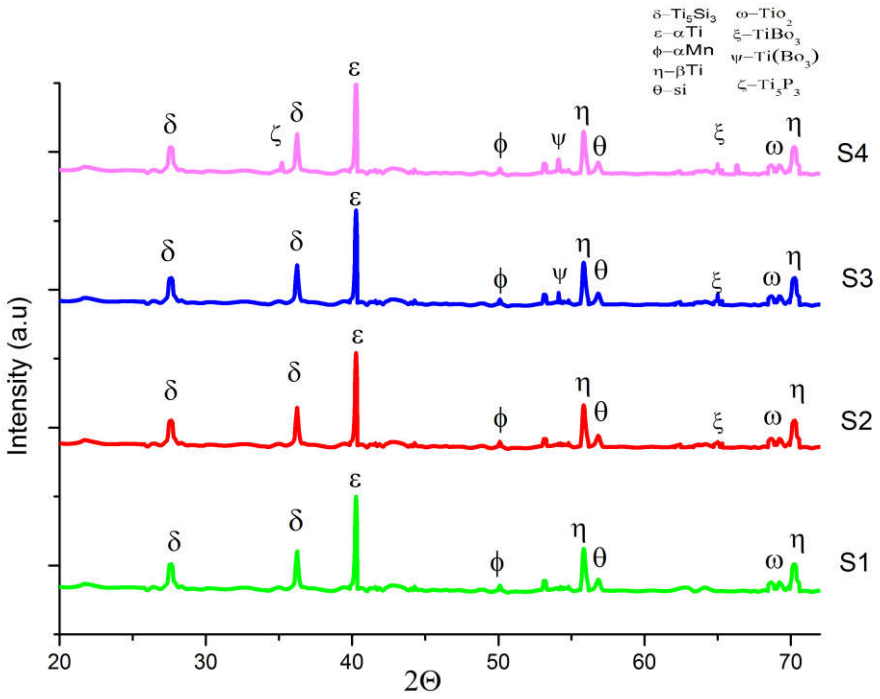

Fig.4.1 XRD spectra of composites containing 1393 B3 bioactive glass

4.5.2 Scanning Electron Microscopy (SEM)

The SEM micrographs of composites are shown in Fig 4.2, Fig (4.2a) and (4.2b) shows the micrograph of pure alloy phase, where, the structure is plate-like with some sort of brittle intermetallic compound between them. The plate-like structure (Yellow arrow) is due to the fact that during ball mill, material suffers random collision with steel balls and become flattered (plate-like) due to the ductility of metals.

The lower amount of glassy phase (Red arrow) which encapsulates the alloy (S2) is also visible in microstructures 2c and 2d where the reinforcement of BAG is small (5%). Figure 4.2 (e, f, g, h) reveal that the alloy particles are embedded more in the glassy phase as the percentage of bioactive glass changes from 10% (S3) to 20 % (S4). The more embedded metal particles in glassy phase signify the homogeneous distribution of melted glass on the surface of the composite. The enhanced non-homogenous pores (Blue arrows) having

approx. 80-110 µm sizes with the reinforced percentage of bioactive glass are also clearly visible in micrographs.

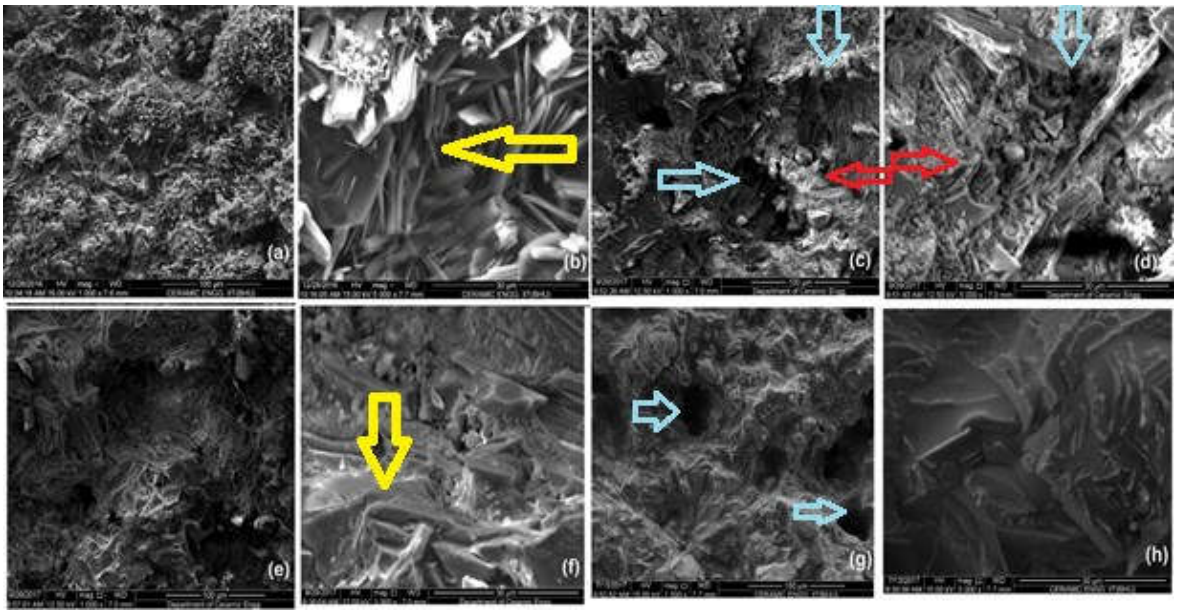

Fig.4.2 SEM micrographs of (a,b) pure alloy S1 (c,d)Alloy + 5%BAG S2 (e,f) Alloy +10%BAG S3 (g,h)Alloy + 20%BAG S4

4.5.3 Physio-mechanical Properties

Fig 4.3 (a) and 4.3 (b) shows apparent porosity and bulk density of the samples respectively. With the increasing amount of bioactive glass from 5% to 20%, the porosity of the synthesized porous samples increases while bulk density decreases. The maximum porosity i.e. 22 % is obtained from the reinforcement of sample containing 20 % of bioactive glass. This can be attributed to the increase in weight percentage of bioactive glass that replaces the Ti alloy matrix.

A conceivable reason for this behavior is that when bioactive glass replaces the original alloy matrix in composite, interplay between particles of glass and alloy at interface increases. A little proportion of the reinforcing phase may occupy the internal voids of

alloy matrix easily, so the densification affects by smaller amounts but as the percentage of reinforcement increases, the internal friction and resulting bridging effect during single-action pressing effectively suppresses the densification [18, 19]. This leads to lower density of the composites. The SEM micrographs (Fig 4.2) also confirm the discussion given above.

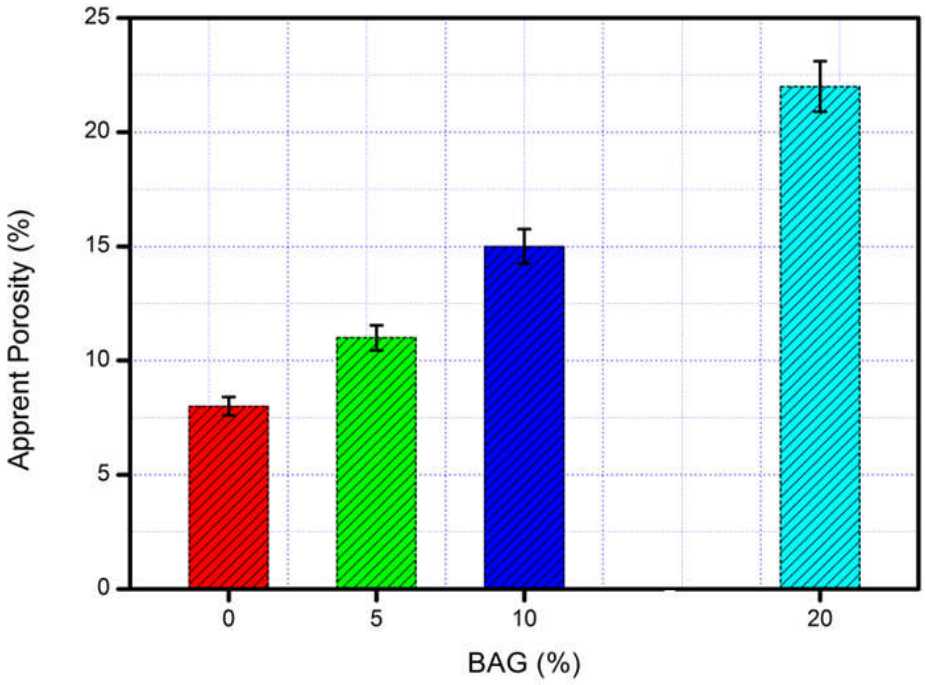

Fig.4.3 (a) Apparent porosity of all the samples (S1, S2, S3, S4)

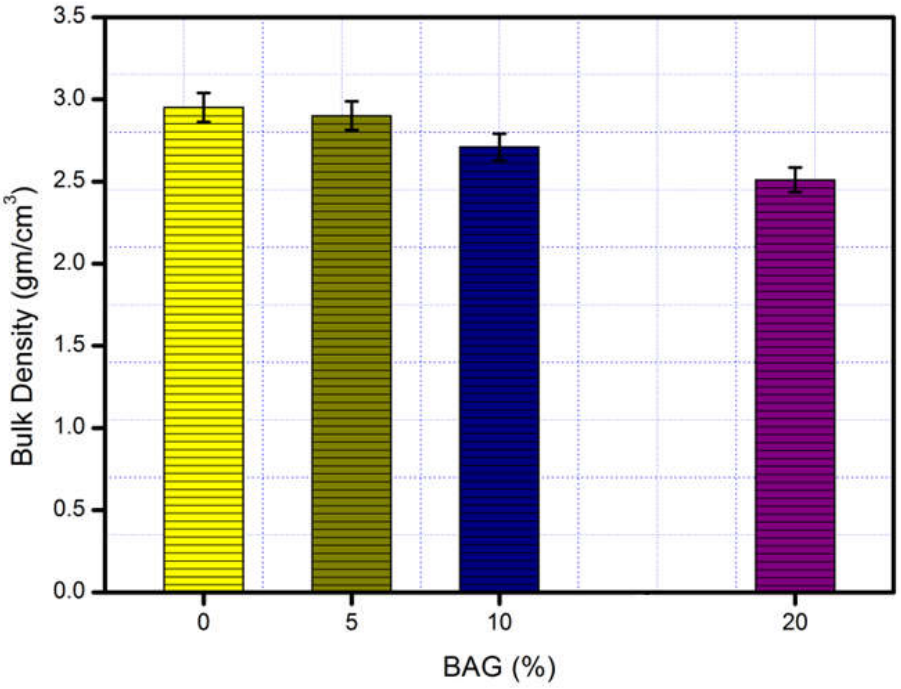

Fig.4.3 (b) Bulk Density of all the samples (S1, S2, S3, S4).

The results of Vickers's hardness measurement of the reinforced alloy are shown in figure 4.4. The hardness of pure alloy matrix (S1) increases (422 Hv) as compared to commercial pure Ti and Ti6Al4V alloy because of the formation of intermetallic compounds in the composite. Further, the graph also reveals that hardness decreases with the reinforced percentage of bioactive glass, reaching to the value of 358 Hv at 20% of reinforcement but it is still superior to the hardness of the cortical bone [40].

Although the amount of intermetallic component increases in composites S2, S3, and S4 which would have raised the hardness of the composites but due to increased porosity, the hardness decreases.

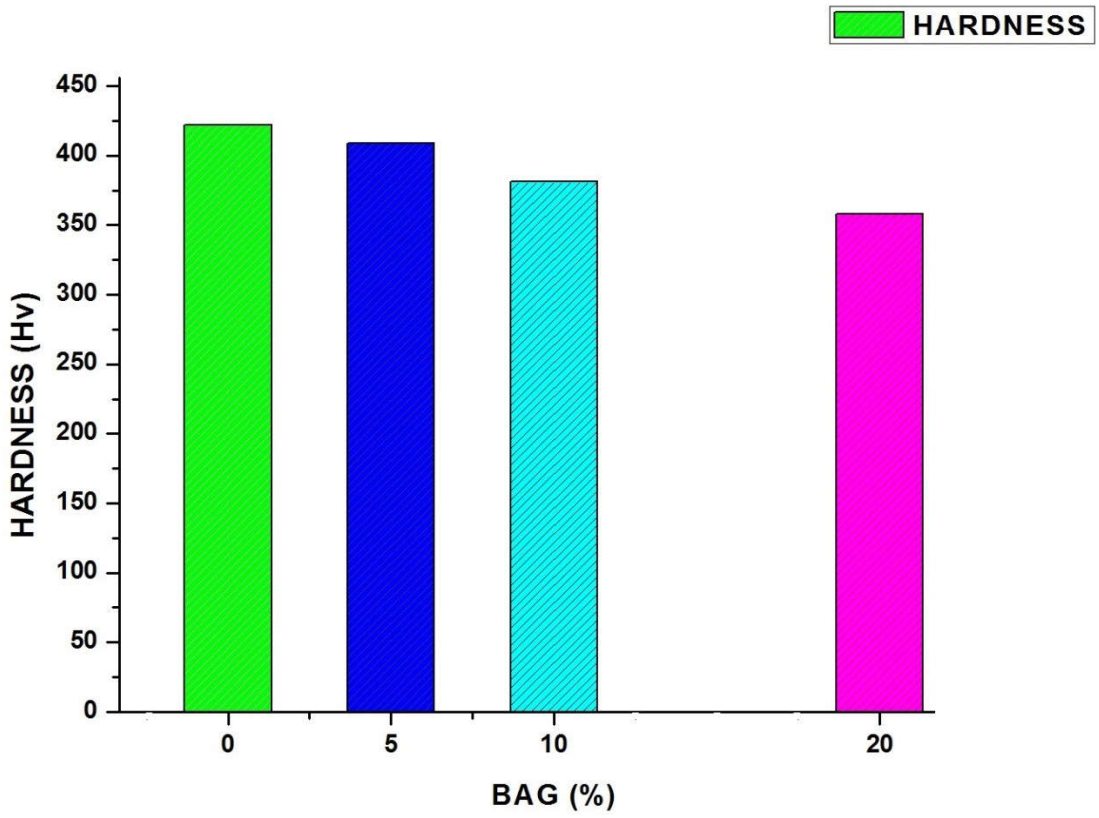

Fig.4.4.Vickers's Hardness of all the samples (S1, S2, S3, and S4)

The measured elastic modulus of prepared composites is represented in fig.5. It shows that the pure alloy matrix (S1) possesses the elastic modulus of 97 GPa which is lower than the commercially available Ti-6Al-4V alloy (110 GPa) [41]. Fig. 5 also shows the modulus value decreases on increasing the reinforcement of 1393 B3 bioactive glass. The value reaches up to 68 GPa at 20 % reinforcement which is an essential requirement of the implant to minimize the stress shielding effect [42].

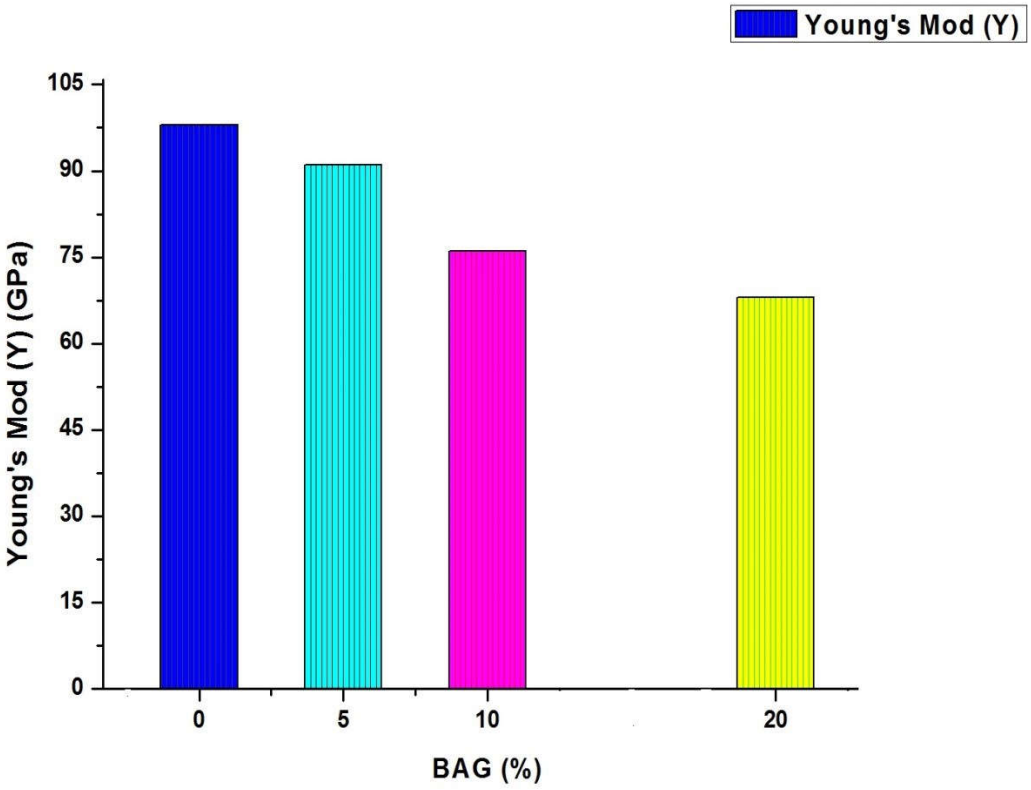

Fig.4.5 Elastic Modulus of all the samples (S1, S2, S3, and S4)

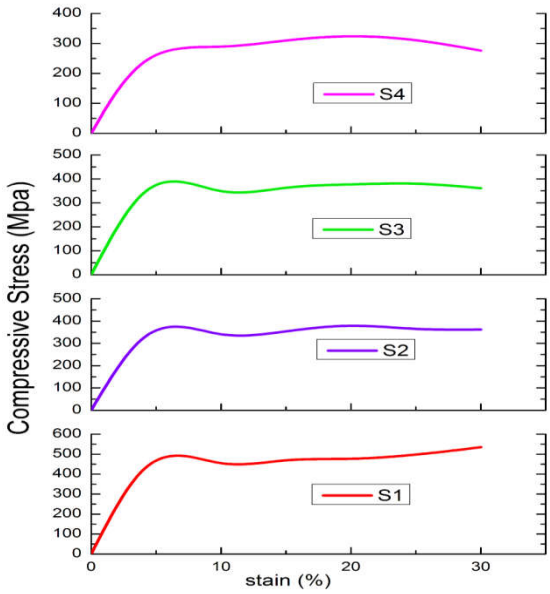

Fig. 4.6 (a) Compressive Stress-Strain relationship for all the samples.

Fig 4.6 (a) shows the stress-strain relationship for the different composites for the compressive strength measurement. The corresponding compressive strengths of different samples in relation to the reinforcement percentage are depicted in fig 6 (b). Compression tests were performed up to the strain value of about 30%. Fig 6(b) shows that the pure alloy matrix (S1) has the maximum compressive strength of 418 Mpa which decreases up to 318 Mpa (S4) with the increased porosity, even though, it is superior to the human cortical bones [43].

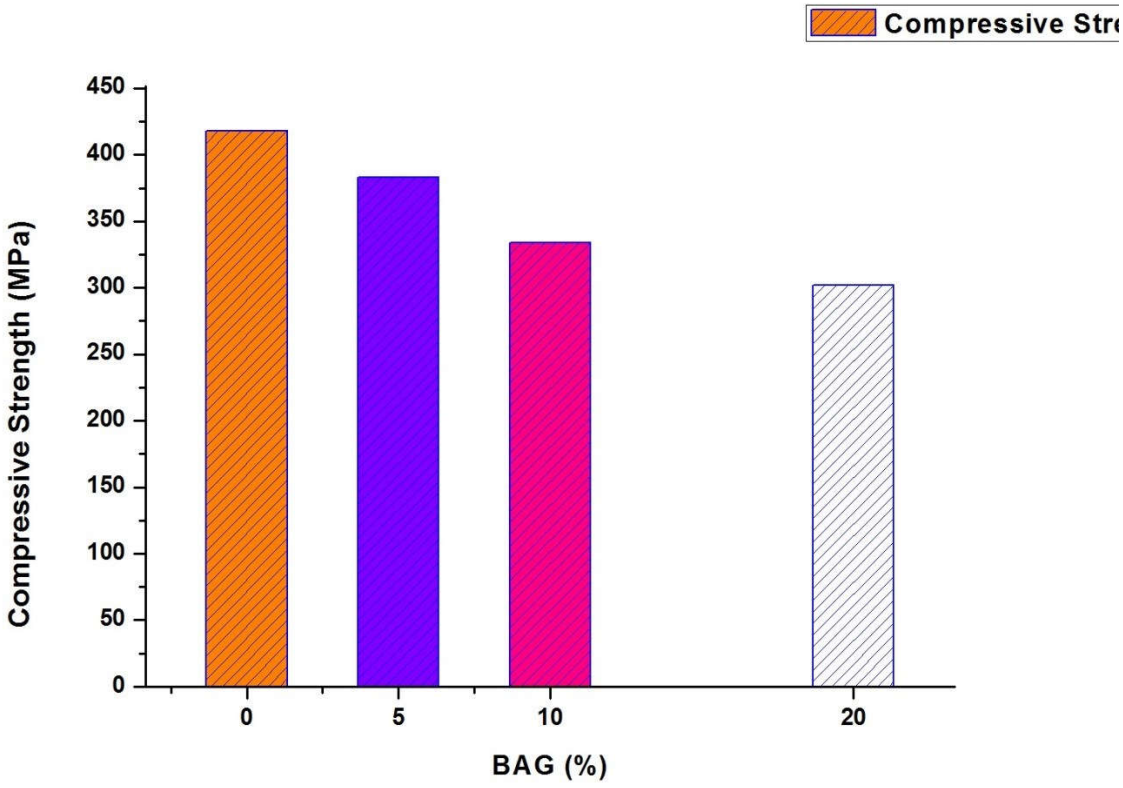

Fig. 4.6 (b) Compressive Strength of all the samples (S1, S2, S3, and S4)

4.5.4 In vitro Bioactivity

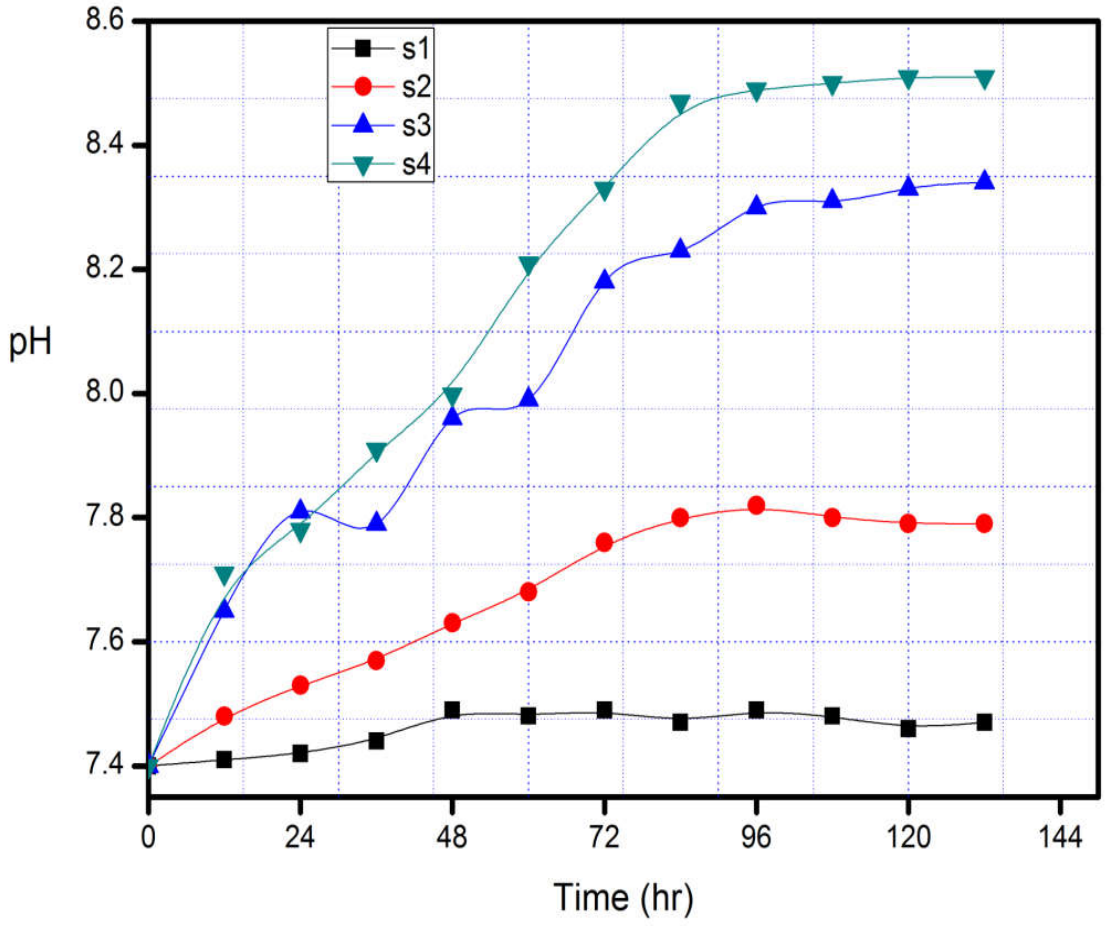

Fig. 4.7 Variation of pH for all samples with respect to the immersing time

To analyze the formation of hydroxyl carbonated apatite (HCA) layer on immersing the samples in SBF solution, the pH behavior of SBF solution has been noted down during different immersion time. Figure 4.7 shows the change of pH in different immersion time up to 5 days. It is clear from the graph that the pH value of all the composite samples (S2, S3, S4) except for S1, increases to 7.82, 8.30, 8.49 respectively within five days as compared to the initial pH (7.4) of SBF solution at 370C under physiologic conditions.

The increase in pH in composites S2, S3 and S4 illustrate the dissolution of cations i.e boron ions and the network modifiers (such as Na+ and K+) from the surface of the glass [44]. The different value of pH after 5 day for the S1, S2 and S3 composites are due to the

difference in weight percentage of bioactive glass in the composition. These cations from the glass along with the phosphate ions released from the SBF solution give rise to the formation of the hydroxyl appetite layer [45].

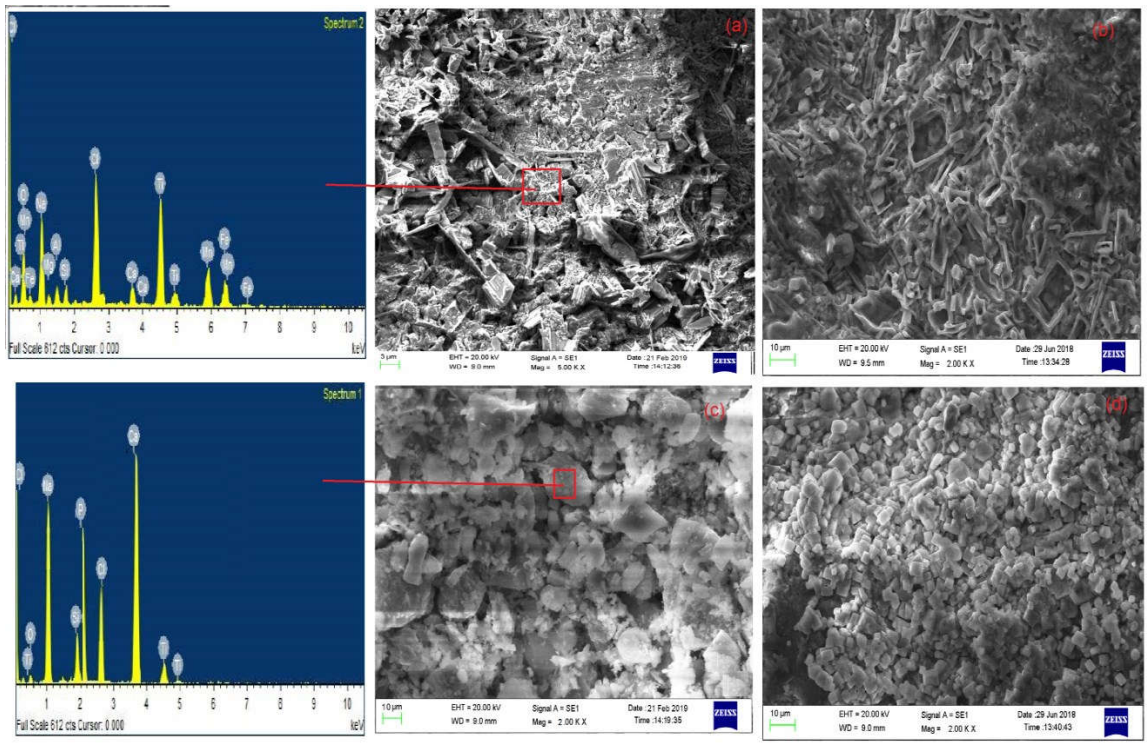

Fig.4.8 SEM of (a) sample S1 (b) sample S2 (c) sample S3 (d) sample S4 (e) EDS spectra of S1 (f) EDS spectra of S3 after immersion in SBF for 5 days.

Table 4.1. EDS elemental analysis of sample S1 and S3 after immersion in SBF

Elements (Weight %)	Ca	Na	P	Cl	O	Si	Ti	Mg	Al	Fe	Mn
S1	2.09	13.33	1.1	12.46	31.41	1.59	17.28	1.32	1.56	7.66	10.20
S3	29.00	24.60	19.00	11.00	08.40	04.20	03.80	--	--	--	--

The graph also depicts that the rate of change of pH also increases with the reinforcing percentage of 1393 B3 bioactive glass. The growth of hydroxyl carbonated apatite layer formed on the surface of samples can also be seen in SEM micrographs which are taken after five days of immersion (fig 4.8). The change of morphologies is seen in the micrographs when compared with the initial surface of samples (fig 4.2). The EDX spectra of S1 and S3 samples are shown in Fig 4.8 (e) and 4.8 (f) respectively, and the corresponding elemental analysis was given in Table 2, which indicates the presence of Ca, P, Na, Cl, Si, and Ti element on the surface of the samples. The Ca to P ratio in the layer formed on the surface of the S3 sample calculated from table 2 is 1.52 which further confirms the formation of HCA layer on the surface. Fig 8 also shows that the irregular shape of carbonated-hydroxyl apatite on the surface of the samples and as the percentage of bioactive glass increases in samples from 5 % to 20%, crystallization of HCA particles are grown better in the form of agglomerates.

4.5.5 Cell culture

Human osteosarcoma cells U2-OS were procured from American Type Culture Collection (ATCC), Manassas, USA and was maintained in RPMI 1640 (Invitrogen, Carlsbad, CA), supplemented with 10% fetal bovine serum (Hyclone, Logan, UT), 100 U/ml penicillin and 100 µg/ml streptomycin (Invitrogen, Carlsbad, CA), henceforth considered as complete medium.

Treatment of U2-OS cells with the increasing concentration of the compound S1, S2, S3, and S4 shows a dose-dependent augmentation of the cytotoxicity in the tumor cells (Fig.4.9 A-D). Among the products, S1 and S3 are more tolerant compared to the other two formulations. Comparative analysis of the cytotoxicity at concentrations of 25 and 100 µg, suggests that the compounds at a higher level are severely toxic to the cells and only relatively safe at the lower concentration tested.

4.5.6 Statistical analysis

For the comparison between the groups, unpaired student's t-test or one way ANOVA followed by Tukey's post hoc test have been used. The data represented as mean ± SD (standard deviation) and the test was conducted three times for each sample. The significant differences were considered for ‘p’ value < 0.05. $p< 0.001$ (****).

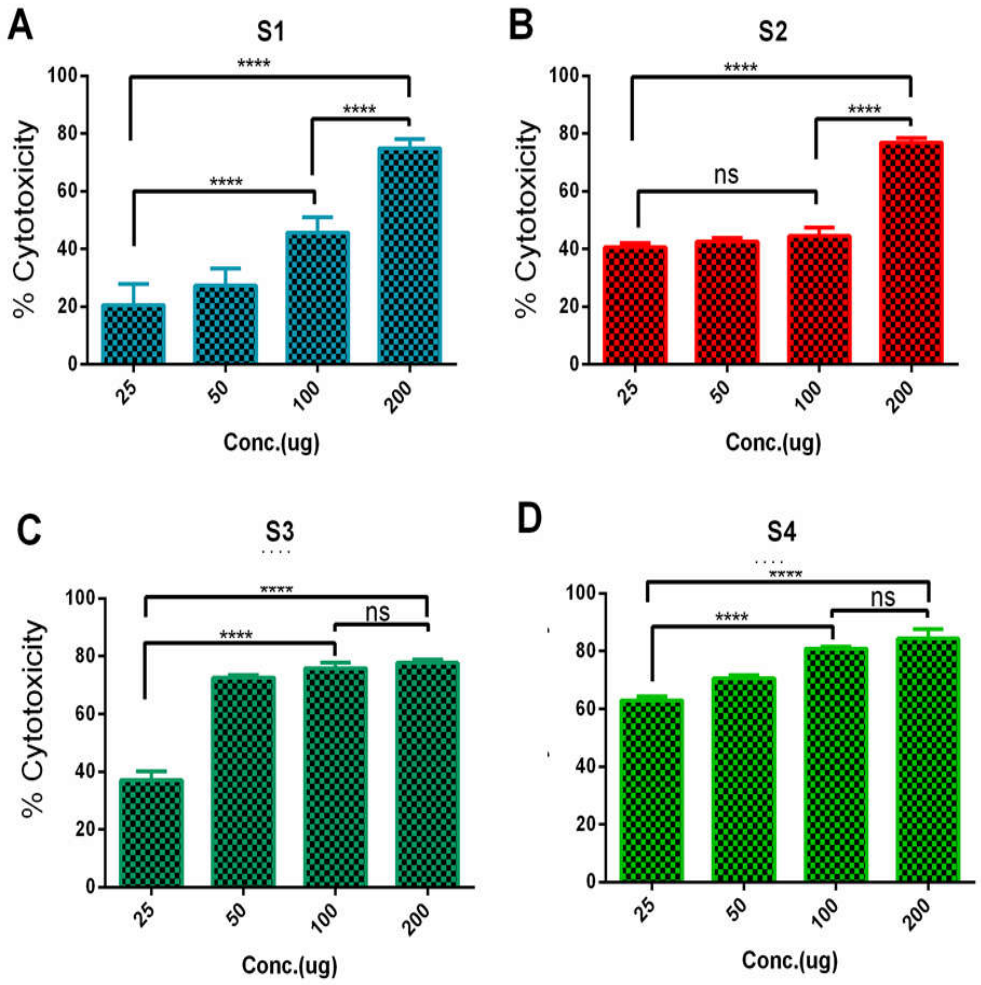

Fig.4.9. The concentration-dependent killing of the U2-OS cells in the presence of S1, S2, S3, and S4.

We tested the proliferation of the cells in the presence of varying concentration of the above compounds. Our data suggested that compound S1 and S3 supports the growth of the tumor cells at a concentration of 25 µg (Figure 4.10). However, both S2 and S4 are not tolerant to the tumor cells and hinder the proliferation of the cells. Increasing the concentration of the compound largely detrimental for the tumor cells growth for all the compounds tested (Figure 4.10).

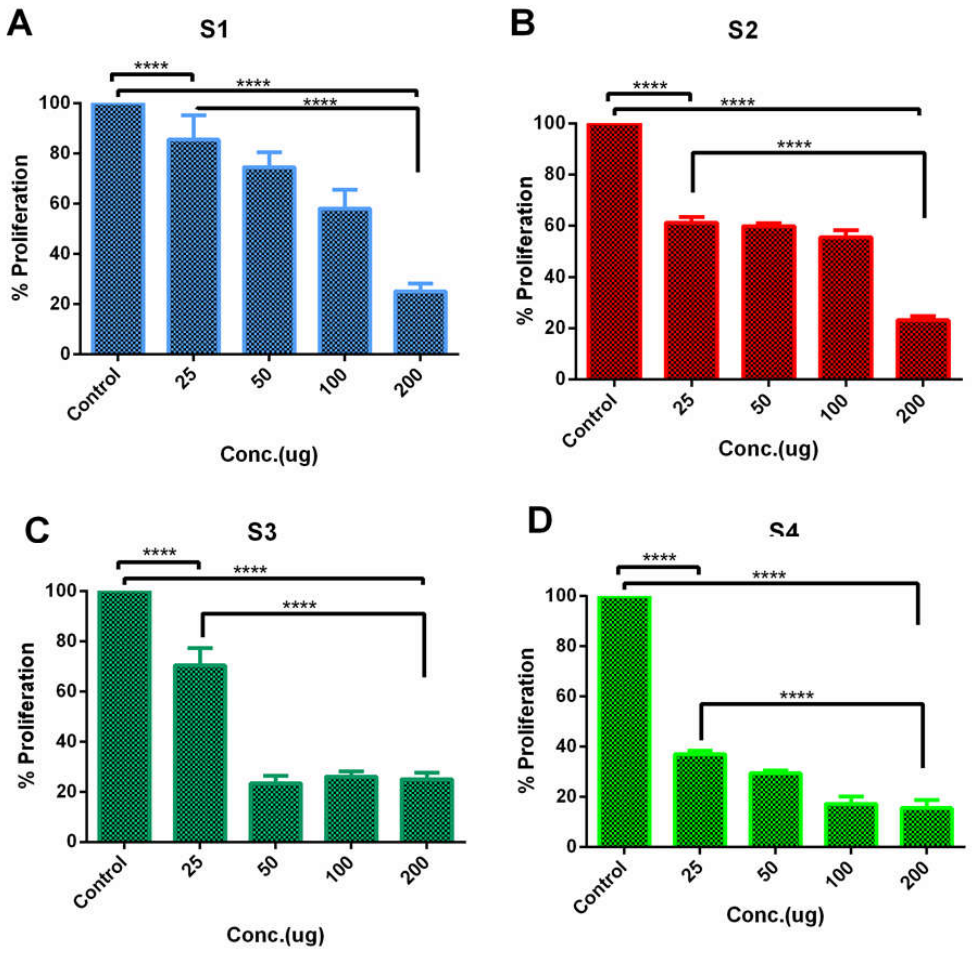

Fig.4.10. The effect of different concentration of S1, S2, S3, and S4 on the proliferation of the U2-OS cells

From the above results, it is clear that compounds are relatively safe at low concentration; however, at higher concentration the formulations may be detrimental for the cells.

Besides the concentration-dependent kinetics, we have also performed time-dependent effect of a fixed concentration of the alloy/BAG complex against the U2-OS cells. At a concentration of 100 µg, the effect of the alloy/BAG complex was studied up to 72 hours. Our data suggested that as time progresses, the proliferation of the cells in the presence of the compound was affected.. The effect of the compounds on the dividing cells like U2-OS

indicates that the alloy/BAG complexes are relatively tolerant to the cells and the compounds are cytocompatible (Fig 4.11). This also suggests that the compound may be used for the implant since osteocytes like U2-OS are present in association with bone tissues where the possible implantation could be made. This indicates that the compound may be biologically compatible for real-life scenario.

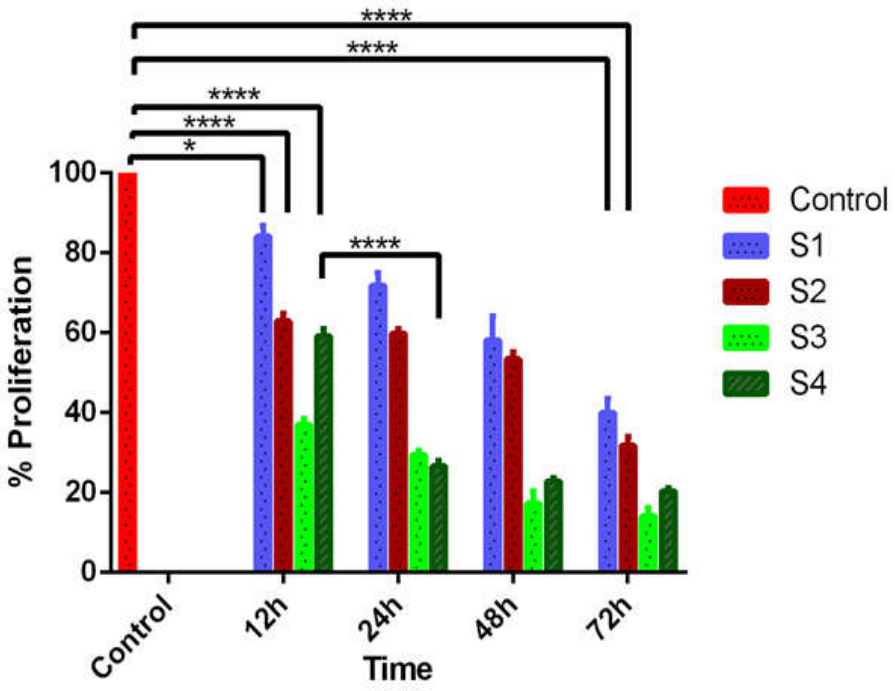

Fig 4.11. Time dependent proliferation of the U2-OS cells at fixed concentration (100 mg) of S1, S2, S3 and S4

4.6 Corrosion Study

The corrosion study has been carried out from weight loss method to study the effect of SBF on the prepared samples. Fig 4.12 depicts the relation between the corrosion rate of tested samples and immersion time. This graph shows that the composites S2, S3, and S4 comprise 1393 B3 BAG initially have a high corrosion rate as compared to pure alloy S1.

This is probably because of the fast degradation rate of borate bioactive glass which leads to the weight loss of the samples [46]. Due to this fact, initially the corrosion rate becomes high, but as the time passes, the rate of weight loss decreases and hence the corrosion rate decreases and approaches nearly to .0015 millimetre per year (mmpy).

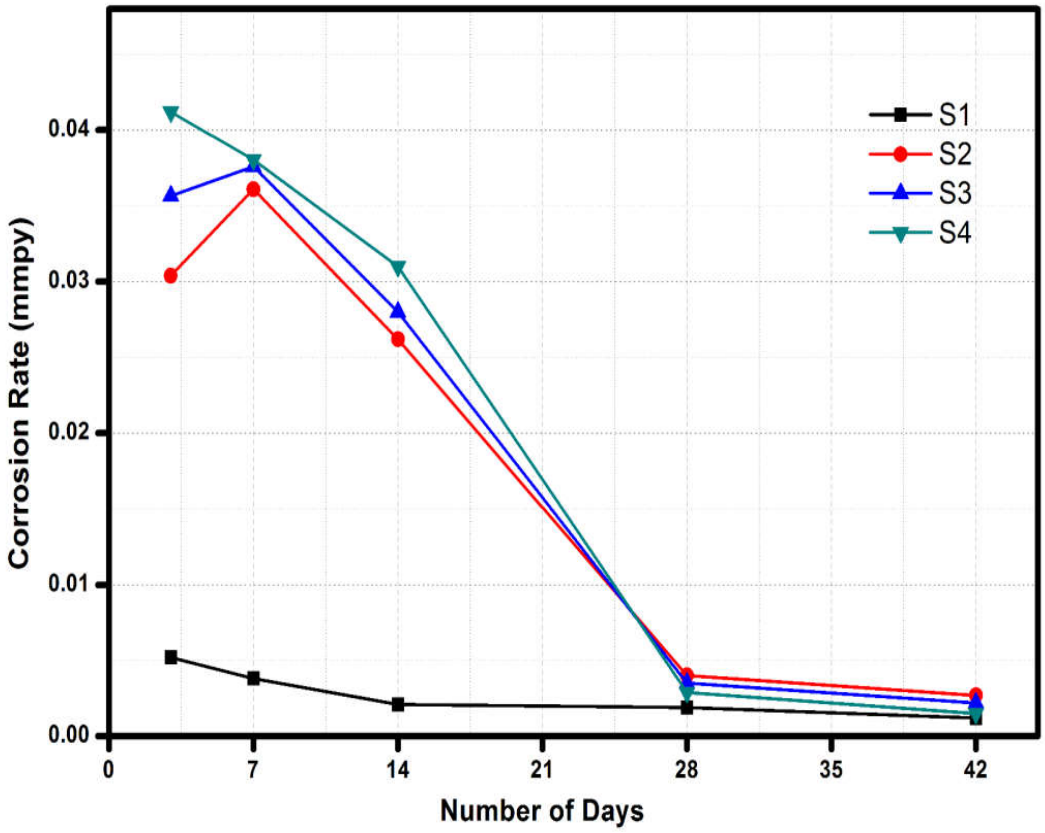

Fig.4.12 corrosion rate of pure alloy (S1) and all composites containing BAG (S2, S3, S4)

4.5. Conclusions

The effect of reinforcement of bioactive glass on the physical, mechanical, biological and corrosion properties of the biomedical composite was investigated and led to the following findings.

1. With the increased percentage of 1393 B3 bioactive glass, the porosity of composites increases and attain the value of 11% (S2), 15%(S3) and 22% (S4) due to the friction between glass and alloy particles at the interface which will be beneficial in the biological fixation and Osseointegration.

2. The Hardness of pure alloy S1 (422 Hv) increases as compared to Ti-6Al-4V alloy because of inclusion of intermetallic and decreases with an increasing percentage of reinforcement due to increasing porosity. However, the respective harnesses are still comparable to cortical bone and Ti-6Al-4V reported in the literature.

3. Among the studied samples, S3 and S4 exhibit the significant reduction in Young's modulus (76 and 68 Gpa) as compared to the reported modulus (110 Gpa) of Ti-6Al-4V alloy. This lower value of Young's modulus comes much closer to that of cortical bones which will be beneficial to reduce the stress shielding effect between implant and bone.

4. The compressive strength of pure alloy S1 is 418 Mpa. The addition of bioactive glass 05% BAG (S2), 10%BAG (S3) and 20% BAG (S4) give the compressive strength of 323, 339 and 318 Mpa respectively which are superior to cortical bone.

5. HCA layer formation in SBF is more prominent in S3 and S4 composite where the reinforcement percentage reaches 10 % and 20 % respectively.

6. The cell culture including cytotoxicity and proliferation essay suggest that composite S1 and S3 are biocompatible and support the growth of the tumor cells at a lower concentration.

7. Composites having bioactive glasses initially have a high rate of corrosion in SBF due to the degradation of borate glass, and as degradation slows down, the corrosion rate reaches to the .0015 mmpy making the composite suitable for permanent implant.

The above results infers that Composite S3 having 10 % reinforcement of 1393 B3 bioactive glass in Ti-8Si-2Mn alloy matrix comes out to be optimized composition because of greater mechanical properties i.e. superior compressive strength (339 MPa), low Young's modulus (76 GPa), optimum density (2.71 gm/cm3) and hardness (381 Hv) as compared to pre-existing Ti implants and more closely matched mechanical and biological properties with that of cortical bone. So it can be proposed as a new novel load bearing bio implant which will potentially reduce the stress shielding effect, toxicity and will improve the Osseo conductivity.

References:

[1] M. Dekker, Manganese and its role in biological process "METAL IONS IN BIOLOGICAL SYSTEMS" edited by Astrid Sigel and Helmut Sigel. 2000; 7:3.

[2] Santamaria AB, Manganese exposure, essentiality & toxicity. The Indian Journal of Medical Research 2008; 128: 484–500.

[3] Li Y, Lee I, et al. The biocompatibility of nanostructured calcium phosphate coated on micro-arc oxidized titanium. Biomaterials 2008; 29: 2025–2032.

[4] SilviaSprianoa, SeijiYamaguchi et al. A critical review of multifunctional titanium surfaces: New frontiers for improving osseointegration and host response, avoiding bacteria contamination. Acta Biomaterialia 2018; 79:1-22.

[5] Yang CY, Chang E, Bond degradation at the plasma sprayed HA coating /Ti--6AI-4V alloy interface: an in vitro study, Journal of materials science: materials in medicine. 1995; 6:258-265.

[6] Julian R. Jones, Alexis G. Clare Bio-Glasses- An Introduction chapter 2, (2012) John Wiley and Sons, Ltd. willey

[7] Tripathi H, Rath C, et al. Structural, physico-mechanical and in-vitro bioactivity studies on SiO2–CaO–P2O5–SrO–Al2O3 bioactive glasses. Materials Science & Engineering C. 2019; 94: 279–290.

[8] Tripathi H, Kumar S, et al. Structural characterization and in vitro bioactivity assessment of SiO 2 – CaO – P 2 O 5 – K 2 O – Al 2 O 3 glass as bioactive ceramic material. Ceramics International 2015 41: 11756–11769.

[9] Tripathi H, Kumar AS, et al. Preparation and characterization of Li2O – CaO – Al2O 3 – P2O5 – SiO2 glasses as bioactive material. Bull. Mater. Sci. 2016; 39: 365–376.

[10] Hirao K, Zhang Z, et al. Hirokazu Morita, Naohiro, Effect of densification treatment on the mechanical properties of borate glasses, Soga. Journal of the Society of Materials Science Japan 451; 40:400-404.

[11] Rahaman MN, Bioactive ceramics and glasses for tissue engineering, in: Aldo R Boccaccini, P.X. Ma. Tissue Engineering Using Ceramics and Polymers wood head publishing 2014.

[12] Nouri A, Wen C, Surfactants in Mechanical Alloying / Milling : A Catch-22 Situation Critical Reviews in Solid State and Materials Sciences 2014; 39:81-108.

[13] Loop W, Standard Test Method for Water Absorption, Bulk Density, Apparent Porosity, and Apparent Specific Gravity of Fired White ware Products 2018; 88: 1–2.

[14] Kokubo T, Kushitani H, et al. Solution to reproduce in vivo surface-structure changes in bioactive glass-ceramic A-W3. J of Biomedical Materials Research 1990;24: 721–734.

[15] Gardner S. Haynes, Laboratory Corrosion Tests and Standards, American Society for Testing and Materials 1985; 04: 529.

[16] Hira SK, Ramesh K, et al. Methotrexate-Loaded Four-Arm Star Amphiphilic Block Copolymer Elicits CD8 + T Cell Response against a Highly Aggressive and Metastatic Experimental Lymphoma. ACS Applied Materials & Interfaces 2015; 7: 20021–20033.

[17] Hira, S. K.; Mishra, A. K.; Ray, B.; Manna, P. P. Targeted delivery of doxorubicin-loaded poly (epsilon-caprolactone)-b-poly (Nvinylpyrrolidone) micelles enhances antitumor effect in lymphoma. PLoS One 2014; 9: e94309

[18] Dai LH, Ling Z, et al. Size-dependent inelastic behavior of particle-reinforced metal - matrix composites. Composites Science and technology 2001; 61: 1057–1063.

[19] Su Y, Ouyang Q, et al. Composite structure modeling and mechanical behavior of particle reinforced metal matrix composites. Materials Science & Engineering A. 597 (2014) 359–369.

[20] Weaver J K, et al. The microscopic hardness of Bone. J Bone Joint Surg 1966; 48 A (2):273-88.

[21] Niinomi M, Recent research and development in titanium alloys for biomedical applications and healthcare goods. Scie. and Tech. of Adv. Matt. 2003; 4: 445–454.

[22] Osamu O, Akira S, Ishi M, Fundamental Study on Titanium Alloys for Dental Castin. The Japanese Society for Dental Materials and Devices (JSDMD) 1985; 4: 708 -715

[23] C. Cases, Implant biomaterials: A comprehensive review World Journal of Clinical Cases .2015; 3(1):52-57.

[24] Geetha M, Singh AK, et al. Ti based biomaterials, the ultimate choice for orthopaedic implants-A review. Progress in Materials Science. 2009; 54: 397–425.

[25] Sennerby L, Thomsen P, et al. A morphometric and biomechanic comparison of titanium implants inserted in rabbit cortical and cancellous bone. The International Journal of Oral & Maxillofacial Implants. 1992; 7:62–71.

[26] Walker PR, LeBlanc J, Sikorska M, Effects of aluminum and other cations on the structure of brain and liver chromatin. Biochemistry 1989; 28: 3911–3915.

[27] Rao S, Ushida T, et al. Effect of Ti, Al, and V ions on the relative growth rate of fibroblasts (L929) and osteoblasts (MC3T3-E1) cells. Bio-Medical Materials and Engineering. 1996, 6:79–86.

[28] Gomes C C, Moreira LM, et al. Assessment of the genetic risks of a metallic alloy used in medical implants. Genetics and Molecular Biology 2011; 34: 116-121.

[29] G.S. Leventhal, TITANIUM, A METAL FOR SURGERY, J. Bone Joint Surg.2006; 33: 473–474.

[30] Li Y, Yang C, et al. New developments of ti-based alloys for biomedical applications. Materials 2014; 7: 1709–1800.

[31] Ho WF, Ju CP et al. Structure and properties of cast binary Ti-Mo alloys. Biomaterials 1999; 20: 2115–2122.

[32] Ho WF, A comparison of tensile properties and corrosion behavior of cast Ti – 7. 5Mo with c. p. Ti, Ti – 15Mo and Ti – 6Al – 4V alloys. J of Alloys and compounds 2008; 464: 580–583.

[33] Ho WF, Chiang TY, et al. Mechanical properties and deformation behavior of cast binary Ti – Cr alloys. J of Alloys and compounds 2009; 468: 533–538.

[34] Ho WF, Chiang TY, et al. Evaluation of low-fusing porcelain bonded to dental cast Ti – Zr alloys. J of Alloys and compounds 2009; 471: 185–189.

[35] Ho WF, Wu S, et al. Evaluation of the machinability of Ti – Sn alloys. J of Alloys and compounds 2010; 502: 112–117.

[36] Hsu HC. Lin HC, Microstructure and grind ability of as-cast Ti – Sn alloys. J Matt Sci 2010; 45: 1830–1836.

[37] Ho WF, Cheng CH, et al. Evaluation of low-fusing porcelain bonded to dental cast Ti – Zr alloys. J of Alloys and compounds.2009; 471: 185–189.

[38] Wang P, Feng Y, et al. Microstructure and mechanical properties of Ti – Zr – Cr biomedical alloys. Materials Science & Engineering C. 2015; 51: 148–152.

[39] Lautenschlager EP, Monaghan P, Titanium and titanium alloys as dental materials. International Dental Journal .1993, 43: 245–253.

[40] Hsu HC, Wu SC, et al. Structure and mechanical properties of as-cast Ti-Si alloys. Intermetallics 2014; 47:11–16.

[41] Elias CN, Lima JHC, et al. Meyers, Biomedical Applications of Titanium and its Alloys.Biological Materials Science 2008; 60(3): 46–49.

[42] Niinomi M, Nakai M, et al. Titanium-based biomaterials for preventing stress shielding between implant devices and bone. Rev International Journal of Biomaterials. 2011; 2011:1-10.

[43] Carter DR, Hayes WC, Bone compressive strength: The influence of density and strain rate. Science New Series 1976; 194: 1174–1176.

[44] Rajkumar G, Aravindan S, et al. Structural analysis of zirconia-doped calcium phosphate glasses. J of Non-Crystalline Solids 2010; 356: 1432–1438.

[45] Silver IA, Deas J, et al. Interactions of bioactive glasses with osteoblasts in vitro : effects of 45S5 Bioglass, and 58S and 77S bioactive glasses on metabolism, intracellular ion concentrations and cell viability. Biomaterials 2001; 22: 175-185.

[46] Lopes PP, Leite BJM, Ferreira, P.S. Gomes, R.N. Correia, M.H. Fernandes, M.H.V. Fernandes, Silicate and borate glasses as composite fillers: A bioactivity and

biocompatibility study, Journal of Materials Science: Materials in Medicine 2011; 22: 1501–1510.